Quantitative optical spectroscopy can identify long-term local tumor control in irradiated murine head and neck xenografts

Karthik Vishwanath
Daniel Klein
Kevin Chang
Duke University
Department of Biomedical Engineering
136 Hudson Hall, Box 90281
Durham, North Carolina 27708

Thies Schroeder
Mark W. Dewhirst
Duke University
Department of Radiation Oncology
201A MSRB I, Research Drive, Box 3455
Durham, North Carolina 27710

Nimmi Ramanujam
Duke University
Department of Biomedical Engineering
136 Hudson Hall, Box 90281
Durham, North Carolina 27708

Abstract. Noninvasive and longitudinal monitoring of tumor oxygenation status using quantitative diffuse reflectance spectroscopy is used to test whether a final treatment outcome could be estimated from early optical signatures in a murine model of head and neck cancer when treated with radiation. Implanted tumors in the flank of 23 nude mice are exposed to 39 Gy of radiation, while 11 animals exposed to sham irradiation serve as controls. Diffuse optical reflectance is measured from the tumors at baseline (prior to irradiation) and then serially until 17 days posttreatment. The fastest and greatest increase in baseline-corrected blood oxygen saturation levels are observed from the animals that show complete tumor regression with no recurrence 90 days postirradiation, relative to both untreated and treated animals with local recurrences. These increases in saturation are observed starting 5 days posttreatment and last up to 17 days posttreatment. This preclinical study demonstrates that diffuse reflectance spectroscopy could provide a practical method far more effective than the growth delay assay to prognosticate treatment outcome in solid tumors and may hold significant translational promise. [DOI: 10.1117/1.3251013]

Keywords: steady state spectroscopy; radiotherapy; Monte Carlo; turbid medium; tissue optics; FaDu; early response.

Paper 09236LR received Jun. 9, 2009; revised manuscript received Aug. 5, 2009; accepted for publication Aug. 26, 2009; published online Oct. 23, 2009.

1 Introduction

Preclinical models are important in the discovery of novel drugs because they enable rapid and systematic evaluation of different combinations of therapy and doses as well as the sequence in which they are administered in a cost-effective manner before proceeding to expensive, time-consuming clinical trials. The standard method for evaluating cancer therapy in preclinical models is the tumor growth delay assay. Growth delay assays monitor tumor growth or regression over relatively long periods of time (weeks to months) to determine whether or not a subject has responded to a particular treatment. Though this method has been valuable, it hides physiological and functional changes that occur within treated tumors, which are likely to have important therapeutic implications. For instance, recent studies that used a vascular disrupting agent to treat cancers showed no impact on tumor growth, although there was substantial damage to tumor microvasculature within a few minutes of administration,[1] leading to near complete necrosis of the central portions of a tumor within hours.[2]

It is well known that physiological changes such as oxygenation, metabolism, and angiogenesis are hallmarks of carcinogenesis and will be altered early in response to cancer therapy.[3,4] In head and neck cancers, tumor hypoxia has been shown to be an important parameter, which strongly influences the efficacy and outcome of both chemotherapy and radiation therapy.[3,5] Previous work has shown that low tumor pO_2 levels in head and neck cancer patients who were treated with radio- and/or chemotherapy had significantly lower locoregional control rates, higher incidences of residual disease after treatment, and lower 5-yr survival, relative to patients with higher[3,6–8] pO_2.

Imaging techniques such as microPET (micro position-emission tomography) and high-resolution MRI (magnetic resonance imaging) can provide valuable insights into tumor physiology, but are not amenable to frequent use in the laboratory and can at best report on events only at selected time points over the course of cancer therapy. These tools could therefore miss opportunistic time points and/or the interaction between key biomarkers that report on the effect of a particular drug. Immunohistochemical assays of tissue biopsies suffer from similar drawbacks, in addition to the fact that biopsies are subject to sampling heterogeneity.

Here, we report on the use of diffuse reflectance spectroscopy (SPX) to nondestructively and rapidly quantify tumor oxygenation *in vivo* as a predictor of tumor response to therapy. We demonstrate in a proof-of-concept study using a

Address all correspondence to: Karthik Vishwanath, Duke University, Department of Biomedical Engineering, 136 Hudson Hall, Box 90281, Durham, North Carolina 27708. Tel: (919) 660-5033; Fax: (919) 684-4488; E-mail: E-mail: kvh1@duke.edu

1083-3668/2009/14(5)/054051/4/$25.00 © 2009 SPIE

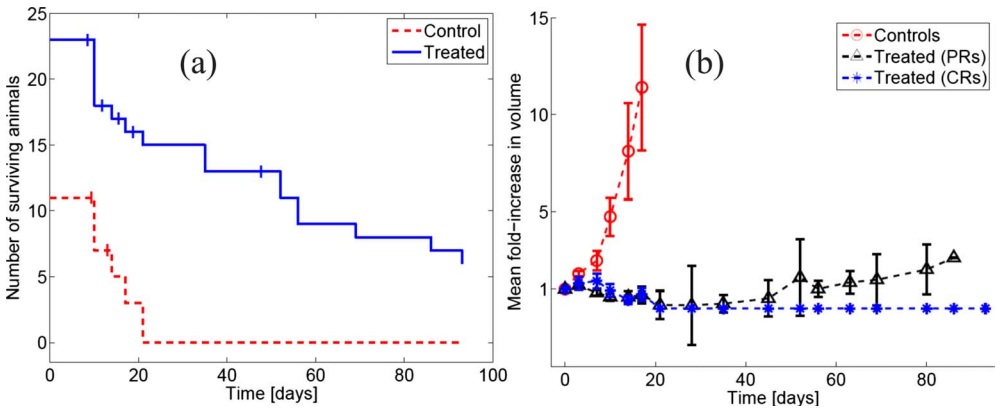

Fig. 1 Number of surviving animals in time in this study. Censored animals are indicated by the vertical ticks at the points of censoring (solid line; treated group, dashed line, control group). (b) Mean fold-increase in tumor volume for the treated (asterisks and triangles) and untreated animals (controls, circles). The treated animals were classified as complete responders (CRs, asterisks) based on the absence of local tumor at the primary site 90 days posttreatment (see text).

nude mouse model of head and neck cancer that this technique can be used frequently and repeatedly to assess tumor oxygenation before, during, and after cancer therapy. We found that the optically estimated tumor oxygen saturation could distinguish between subjects showing partial versus complete response as early as 7 days posttreatment. This tool could augment current growth delay assays and could identify key landmark time points for more detailed assessment with more sophisticated imaging methods and/or immunohistochemistry.

2 Methods

A total of 34 nude mice were inoculated with 10^6 FaDu human hypopharyngeal squamous cell carcinoma cells suspended in 0.1 ml serum-free medium, subcutaneously, on their right flanks. Once the average tumor diameters reached 6 to 8 mm, the animals were evenly distributed by tumor volume into control and treatment groups in a 1:2 ratio, respectively. In the treatment group, $N=23$ animals were exposed to 39 Gy of radiation, while $N=11$ animals in the control group received sham irradiation. The dose of 39 Gy was chosen as it has previously been reported as the TCD_{50} (dose that provides local control to 50% of the treated population) for this tumor model in nude mice.[9] Prior to radiation exposure, all animals (whether treated or shammed) were anesthetized using Nembutal [ip (intraperitoneal) diluted 1:5 by volume] and placed in a custom-built stereotactic holder in the radiation field. Treatment day was labeled day 0. Note that although a single curative dose is not clinically used, this report is an initial study to determine whether (and if so, how early do) optical methods indicate treatment response to radiotherapy.

All tumors were monitored optically before treatment to get baseline measurements on day 0 and then again on days 1, 3, 5, 7, 10, 12, 14, and 17. The animals were anesthetized via Isoflurane breathing (1.5% Isoflurane gas mixed with oxygen) throughout the course of the optical measurements. Tumor volumes were measured once using calipers each day over the course of the optical measurements and then one or two times per week until 90 days posttreatment. The study was approved by the Duke Institutional Laboratory Animal Care and Use Committee.

A fiber-optic-based spectrometer[10] (Skinskan, JY Horiba, Edison, New Jersey) was used to measure the diffuse reflectance in the spectral range between 480 and 650 nm from the FaDu tumors. The illumination and collection of the light to tissue was achieved via a bifurcated fiber optic probe, which at its common end had 40 illumination and 40 collection fibers [each individual fiber was 200 μm in diameter; see Fig. 2(a) in Sec. 3]. This probe was constructed for use with the preceding optical spectrometer and was designed to provide a high enough SNR for a wide range of tissue optical properties using Monte Carlo simulations. Monte Carlo simulations were also used to calculate that the effective penetration depth for this probe geometry was ~0.7–1 mm, for a turbid medium with representative mouse tumor optical properties (with mean absorption coefficient between 480 and 650 nm of 2.8 to 4 cm^{-1} and mean reduced scattering of 15 to 18 cm^{-1}) and indicate that the probe sensed diffuse reflectance signals from depths greater than 0.3 mm, which was the histologically measured mean skin thickness atop these tumors. Two diffuse reflectance scans were consecutively collected from the tumor, at each time point, by gently pushing the probe to make contact with the tumor and fixing it to a clamp so it did not move during the measurements. The acquired diffuse reflectance spectra were calibrated and analyzed using an inverse scalable Monte Carlo model, as described previously,[10] to obtain the wavelength-dependent scattering and absorption spectra. The concentration of oxygenated (HbO_2) and deoxygenated (dHb) hemoglobin in the tumor vasculature was derived from the wavelength-dependent absorption coefficient using the Beer-Lambert equation. Their concentrations were then used to calculate the blood oxygen saturation: $SO_2 = 100 \times HbO_2/(HbO_2 + dHb)$.

3 Results and Discussion

Figure 1(a) shows the number of surviving animals for the treated (solid line) and control (dashed line) over the 90-day period after initiation of treatment. Five control and 7 treated

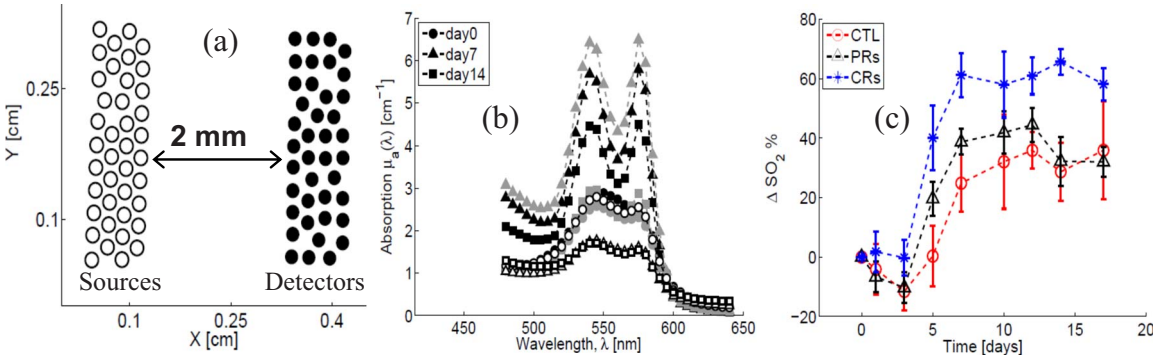

Fig. 2 (a) Fiber optic probe geometry used in this study (open circles indicate source fibers and filled circles represent collection fibers); (b) extracted absorption spectra for one representative animal that was a control (hollow symbols), a PR (gray-filled symbols), and a CR (black-filled symbols) on day 0 (baseline; circles), day 7 (triangles) and day 14 (squares); and (c) average change in tumor blood saturation (relative to day 0, ΔSO_2) for each group (asterisks, CRs; triangles, PRs; circles, controls).

animals were censored due to ulcerations in the tumors before the end of the study and are indicated by the customary vertical ticks in Fig. 1(a). Figure 1(b) shows average fold-increase (relative to baseline) in the tumor volumes for the treated (triangles and asterisks) and the control (circles) animals. The symbols represent the mean value of the fraction increase in tumor volume calculated for all animals that were alive in each group, at each time point, while the error bars represent the standard error. Six of the treated animals showed complete local tumor control with no recurrences up to day 90 (asterisks) and were classified as complete responders (CRs). The remaining 17 treated animals were classified as partial responders (PRs, triangles) since the tumors in these animals recurred locally during the 90-day period (the last recurrence was scored on day 63 posttreatment).

Figure 2(b) shows the extracted absorption spectra on day 0 (circles), day 7 (triangles), and day 14 (squares) for one representative animal from each group (hollow symbols, control; gray fill, PR; black fill, CR). Although the absorption spectra for each of these three animals were quite similar at baseline, we see that the treatment caused an increase in the levels of oxygenated hemoglobin (evidenced through the growth of the characteristic α/β bands of oxyhemoglobin,

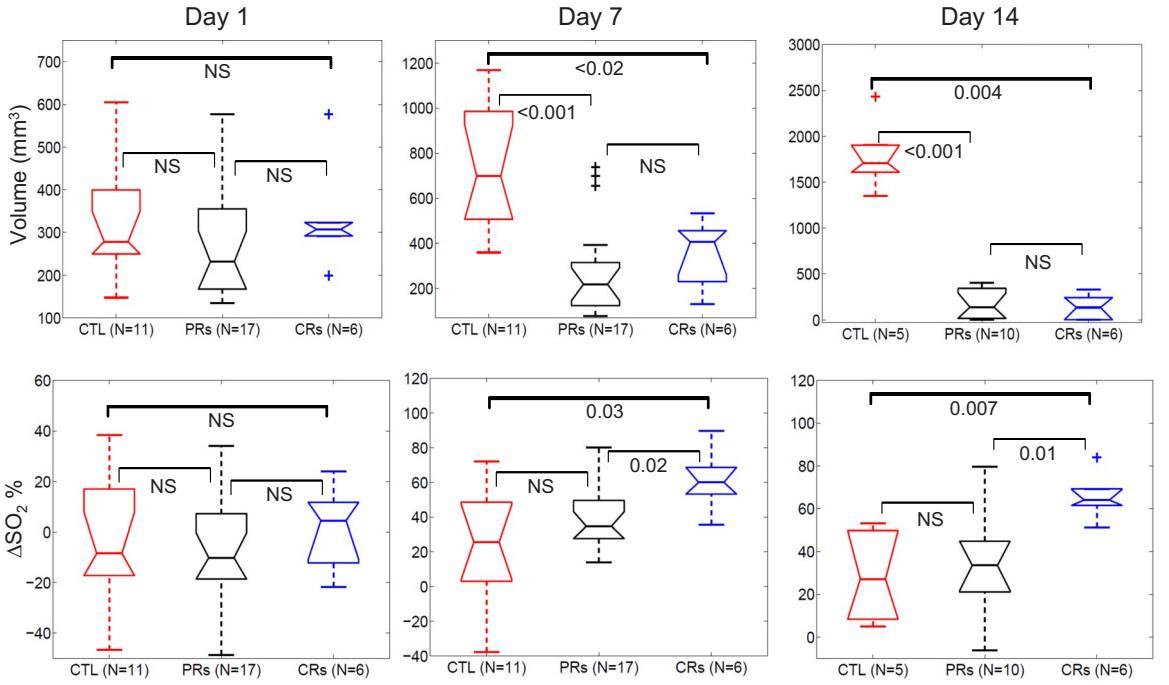

Fig. 3 Comparison of changes in tumor volume [(a) to (c), top row] and ΔSO_2 [(d) to (f), bottom row] across all animals in each group, on days 1, 7, and 14 (columns) using standard box plots. The data between groups were compared using an analysis of variance (ANOVA) for each parameter and day to determine if there were significant differences between the groups, and if so, the groups were compared in a pairwise fashion using the Wilcoxon rank sum test. Each figure shows the p value for all pairwise Wilcoxon comparisons (NS is used to show $p>0.05$), while the x axis labels show the animal numbers and group, for each day (CTL, control).

marked by arrowheads) 7 and 14 days postradiation in the treated animals relative to the controls. Figure 2(c) shows the group averaged time trends in ΔSO_2 for all controls, PRs, and CRs. Here, ΔSO_2 on a given day represents the change in SO_2 on that day relative to the baseline measurement for each animal and enabled comparison of the changes in SO_2 values relative to each subject's baseline. As in Fig. 1(b), symbols represent the mean ΔSO_2 computed across all available animals in each group, at each time point, while the bars are standard errors. Figure 2(c) shows that the tumor oxygen saturation for the CRs (asterisks) had the steepest increase and the highest value relative to the controls (circles) and PRs (triangles) 7 to 14 days posttreatment. The increases seen in the treated groups can be interpreted as a consequence of radiation-induced tumor cell death, which causes a reduced demand for oxygen in the tumors, while the increase in the control group might be a consequence of measuring the increased oxygenated blood (due to inhaled oxygen during anesthesia) that is shunted along the rims in these tumors.[11] We did not, however, observe any significantly distinct trends in the mean optically extracted total hemoglobin values across time between the animals of the three groups.

Figure 3 compares the changes in tumor volume [Figs. 3(a)–3(c)] and ΔSO_2 [Figs. 3(d)–3(f)] across animals in each group, on day 1 [Figs. 3(a) and 3(d)], day 7 [Figs. 3(b) and 3(e)], and day 14 [Figs. 3(c) and 3(f)]. In each plot, the groups (and the number of animals alive for that day) are identified on the x axis labels. Figures 3(a) and 3(d) showed no differences in tumor volumes or ΔSO_2 values between all groups on day 1. By day 7, it was possible to isolate the treated group (both PRs and CRs) from the untreated controls on the basis of an ANOVA test on the tumor volumes, and these differences were maintained on day 14. However, there was no statistically significant difference between the tumor volumes of the PRs and CRs either on day 7 or day 14. The changes in ΔSO_2 on days 7 and 14 for each group, on the other hand, show that the CRs were well separated from both the controls and the PRs, while there was no statistically significant difference between the PRs and control animals, on any of the days.

A previously published report that employed diffuse reflectance spectroscopy to monitor treatment response to photodynamic therapy (PDT) in a murine model of fibrosarcoma observed that an increase in the relative SO_2 (post-versus pre-PDT) was statistically associated with an increased probability of survival without recurrence.[12] Our proof-of-concept study suggests that diffuse reflectance spectroscopy has the potential to differentiate CRs from PRs and nonresponders in preclinical models early in the course of therapy and could therefore be used to rapidly test novel drugs and individualized therapeutic strategies for cancer treatments. Future studies with a larger number of animals will enable us to test the accuracy and efficacy of using optical methods to develop a predictive model to predict/assess treatment outcome.

Acknowledgments

The authors would like to thank Dr. Yulin Zhao for assistance with tumor inoculation. Funding support for this work was provided by the Department of Defense Era of Hope Scholar award (W81XWH-05-1-0363) and the National Institutes of Health Grant No. R01 CA40355-24.

References

1. G. M. Tozer, V. E. Prise, J. Wilson, M. Cemazar, S. Shan, M. W. Dewhirst, P. R. Barber, B. Vojnovic, and D. J. Chaplin, "Mechanisms associated with tumor vascular shut-down induced by combretastatin A-4 phosphate: intravital microscopy and measurement of vascular permeability," *Cancer Res.* **61**, 6413–6422 (2001).
2. S. L. Young and D. J. Chaplin, "Combretastatin A4 phosphate: background and current clinical status," *Expert Opin. Invest. Drugs* **13**, 1171–1182 (2004).
3. J. L. Tatum, G. J. Kelloff, R. J. Gillies, J. M. Arbeit, J. M. Brown, K. S. Chao, J. D. Chapman, W. C. Eckelman, A. W. Fyles, A. J. Giaccia, R. P. Hill, C. J. Koch, M. C. Krishna, K. A. Krohn, J. S. Lewis, R. P. Mason, G. Melillo, A. R. Padhani, G. Powis, J. G. Rajendran, R. Reba, S. P. Robinson, G. L. Semenza, H. M. Swartz, P. Vaupel, D. Yang, B. Croft, J. Hoffman, G. Liu, H. Stone, and D. Sullivan, "Hypoxia: importance in tumor biology, noninvasive measurement by imaging, and value of its measurement in the management of cancer therapy," *Int. J. Radiat. Biol.* **82**, 699–757 (2006).
4. A. A. Neves and K. M. Brindle, "Assessing responses to cancer therapy using molecular imaging," *Biochim. Biophys. Acta* **1766**, 242–261 (2006).
5. H. B. Stone, J. M. Brown, T. L. Phillips, and R. M. Sutherland, "Oxygen in human tumors: correlations between methods of measurement and response to therapy. Summary of a workshop held November 19–20, 1992, at the National Cancer Institute, Bethesda, Maryland," *Radiat. Res.* **136**, 422–434 (1993).
6. M. Nordsmark, S. M. Bentzen, V. Rudat, D. Brizel, E. Lartigau, P. Stadler, A. Becker, M. Adam, M. Molls, J. Dunst, D. J. Terris, and J. Overgaard, "Prognostic value of tumor oxygenation in 397 head and neck tumors after primary radiation therapy. An international multicenter study," *Radiother. Oncol.* **77**, 18–24 (2005).
7. P. Vaupel, A. Mayer, and M. Hockel, "Impact of hemoglobin levels on tumor oxygenation: the higher, the better?" *Strahlenther Onkol.* **182**, 63–71 (2006).
8. D. M. Brizel, R. K. Dodge, R. W. Clough, and M. W. Dewhirst, "Oxygenation of head and neck cancer: changes during radiotherapy and impact on treatment outcome," *Radiother. Oncol.* **53**, 113–117 (1999).
9. C. Petersen, D. Zips, M. Krause, K. Schone, W. Eicheler, C. Hoinkis, H. D. Thames, and M. Baumann, "Repopulation of FaDu human squamous cell carcinoma during fractionated radiotherapy correlates with reoxygenation," *Int. J. Radiat. Oncol., Biol., Phys.* **51**, 483–493 (2001).
10. G. M. Palmer and N. Ramanujam, "Monte Carlo-based inverse model for calculating tissue optical properties. Part I: Theory and validation on synthetic phantoms," *Appl. Opt.* **45**, 1062–1071 (2006).
11. B. S. Sorg, B. J. Moeller, O. Donovan, Y. Cao, and M. W. Dewhirst, "Hyperspectral imaging of hemoglobin saturation in tumor microvasculature and tumor hypoxia development," *J. Biomed. Opt.* **10**, 44004 (2005).
12. H. W. Wang, M. E. Putt, M. J. Emanuele, D. B. Shin, E. Glatstein, A. G. Yodh, and T. M. Busch, "Treatment-induced changes in tumor oxygenation predict photodynamic therapy outcome," *Cancer Res.* **64**, 7553–7561 (2004).